Analysis of Overall Performance of Multi-stage Combustor Scramjet Engine

Jinfeng Du(✉), Chun Guan(✉), Yuchun Chen(✉), Haomin Li(✉), and Zhihua Wang(✉)

School of Power and Energy,
Northwestern Polytechnical University, Xi'an, China
nwpujin@126.com, guanchunl0412@163.com,
chych888@nwpu.edu.cn, 1710274313@qq.com,
wzh0512@mail.nwpu.edu.cn

Abstract. In this paper, based on the scramjet, by the mode of characteristic calculation of one-dimensional scramjet engine, the effect of three and four-section combustion chamber geometry, fuel distribution ratio on scramjet performance is studied. The results of the comparison and evaluation of engine performance provide a certain reference for the geometric configuration of the combustion chamber and fuel injection parameters of the design point. It is mainly to determine the appropriate combustion chamber geometry and fuel injection method to obtain better combustion chamber performance and overall engine performance. The results show that increasing the thermal throat area of the combustion chamber can effectively increase the thrust of the aircraft during low-speed flight condition, and increase the fuel distribution ratio and the length of the expansion section in the front section of the combustion chamber without thermal choke and without affecting the inlet start, can improve the specific impulse of the engine at high speed.

Keywords: Scramjet · Overall performance · Combustion chamber · One-dimensional analysis

Nomenclature

Θ	Attack angle
Ma_0	Flight Mach number
Fn	Thrust
I_{SP}	Specific impulse
Q	Dynamic pressure head
H	Fight altitude (km)
$Width$	The width of the whole aircraft (m)

X. Zhang (Ed.): APISAT 2018, LNEE 459, pp. 1835–1846, 2019.
https://doi.org/10.1007/978-981-13-3305-7_147

1 Introduction

At the beginning of the 21st century, the development of the world's military and war, the high speeds are the preconditions for achieving missile penetration and short-term strategic strikes. Therefore, the development of scramjet technology has become a research hotspot at present. Various countries consider scramjet technology as a key technology in the field of hypersonic research. At present, researchers have carried out a large number of theoretical studies [1–3], numerical simulation studies [2, 3], wind tunnel test studies and flight test studies [4–10].

The United States conducted two consecutive flight tests on the X-43A in 2004 and achieved flight targets of Mach 6.8 and Mach 9.7. On May 1, 2013, NASA completed the scheduled test target, the entire acceleration process lasted for 240 s, flight distance 426 km and no-power gliding (130 s); Japan, Germany, Australia [11–13], etc. are also carrying out their own hypersonic flight test plan. The choice of most propulsion systems is the scramjet engine. It can be seen that the scramjet engine technology has evolved from the theoretical research section of ground tests to the engineering application section.

Wu [14] and Wang [15] considered the design parameters of a three-section expansion type combustor, a single expansion ramp nozzle, and a three-section injection equivalence ratio and corresponding injection when studying scramjet engine combustion chambers. By changing the parameters of the above-mentioned design point, aiming at the maximum thrust and specific impulse, the optimization work is carried out and the test verification is carried out to provide a theoretical basis for the design of the combustion chamber and fuel distribution in the future.

For this reason, the performance of the multi-stage combustion chamber of the scramjet engine is studied in this paper, which provides a basis for future combustion chamber design and fuel distribution.

2 Scramjet Configuration

The working process of the scramjet engine is different from that of the traditional turbine engine. The components in the engine are also different. Therefore, the configuration of the scramjet engine needs to be explained.

2.1 Introduction to the Configuration of the Scramjet Engine

The scramjet engine consists of four parts: the inlet, the isolation, the combustion chamber, the nozzle. Figure 1 shows a schematic diagram of the components of the scramjet. Its cross-section definition and components are as follows (Table 1):

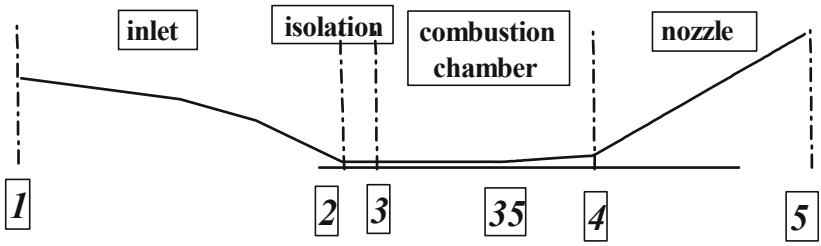

Fig. 1. Schematic diagram of scramjet components

Table 1. Section definition of scramjet

Section marking	Corresponding
Section 1	Undisturbed free flow section
Section 2	Outlet section of inlet/inlet section of isolation
Section 3	Outlet section of isolation/inlet section of first section of combustion chamber
Section 35	Outlet section of first section of combustion chamber/Inlet section of second section of combustion chamber
Section 4	Outlet section of second section of combustion chamber/inlet section of nozzle
Section 9	Outlet section of nozzle

2.2 Introduction to Design Point Operating Parameters of the Scramjet Engine

The engine uses kerosene ($C_{12}H_{23}$) as fuel and multi-point injection (Table 2).

Table 2. Scramjet engine design point parameters

Parameter	Value	Parameter	Value
Wa_0 *(kg/s)*	2.0	*Width (m)*	0.12
Q *(kPa)*	50.0	Ma_0	6.0
Θ (deg)	0	*H (km)*	26.5

3 Influence of Design Parameters of Three Sections of Combustion Chamber

The influence of the parameters of the three-section design of the combustion chamber is studied. Two variables are selected for study: A_{36}/A_3, Φ_2, and the parameters are similarly defined, in which A_{36} is the exit area of the second combustion chamber, and Φ_2 is the fuel supply ratio of the second section of the combustion chamber.

3.1 The Effect of Configuration of the Combustion Chamber

The engine reference configuration remains unchanged, and the expansion ratios of the first and the third sections of the combustion chamber are 1.0 and 2.0, respectively, and the expansion ratio of the combustion chamber in the middle section is A_{36}/A_3 = 1.1 to 1.5, and $\Delta A_{36}/A_3$ = 0.1. The specific profile configuration is shown in Fig. 2. The engine is operated at maximum fuel supply, and the overall performance of the engine at different flight speeds is calculated. The calculation results are shown in Fig. 3.

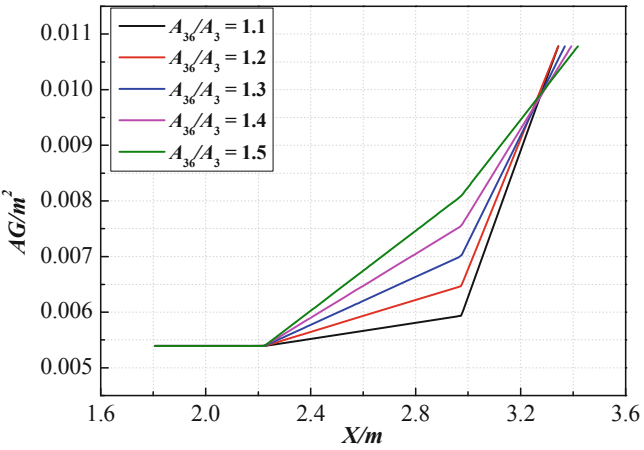

Fig. 2. The configuration of different second expansion ratio in three-section combustion chamber

From Fig. 3(a), we can see that for the same flight condition, when the maximum equivalent fuel-air ratio of the combustion chamber does not reach the equivalent fuel-air ratio Φ = 1.20, the maximum equivalent fuel-air ratio increases with the increase of the second section expansion ratio A_{36}/A_3 of the combustion chamber. This is because the increase in the expansion ratio of the second section of the combustion chamber will lead to an increase in the throat area of the combustion chamber, which will allow more fuel to be added to the combustion chamber. Therefore, at the low Mach number, the maximum equivalent fuel-air ratio in the combustion chamber is large. When the expansion ratio A_{36}/A_3 of the second section of the combustion chamber is constant, with the increase of the flight Mach number Ma_0, the engine thrust appears to increase first and then decrease. The reason is that before the equivalent fuel-air ratio Φ = 1.20, the increase in fuel-air ratio leads to an increase in thrust. The next reduction in thrust is due to the transition of the combustion mode of the engine to the direction of the purely supersonic mode of the boundary layer; for the same flight condition, the maximum equivalent fuel-air ratio in the combustion chamber reaches the equivalent of fuel-air ratio. Before Φ = 1.20, the maximum state thrust increases with the increase of A_{36}/A_3, but when the equivalent fuel-air ratio Φ = 1.20, the thrust decreases with the increase of A_{36}/A_3, but the effect is not significant. The engine specific thrust *Fs* and thrust *Fn*

change trend the same. As can be seen in Fig. 3(d), in general, the specific impulse increases with the increase of A_{36}/A_3 at low Mach number flight, while at high Mach numbers, the specific impulse decreases with the increase of A_{36}/A_3, and the impact of A_{36}/A_3 is getting smaller and smaller.

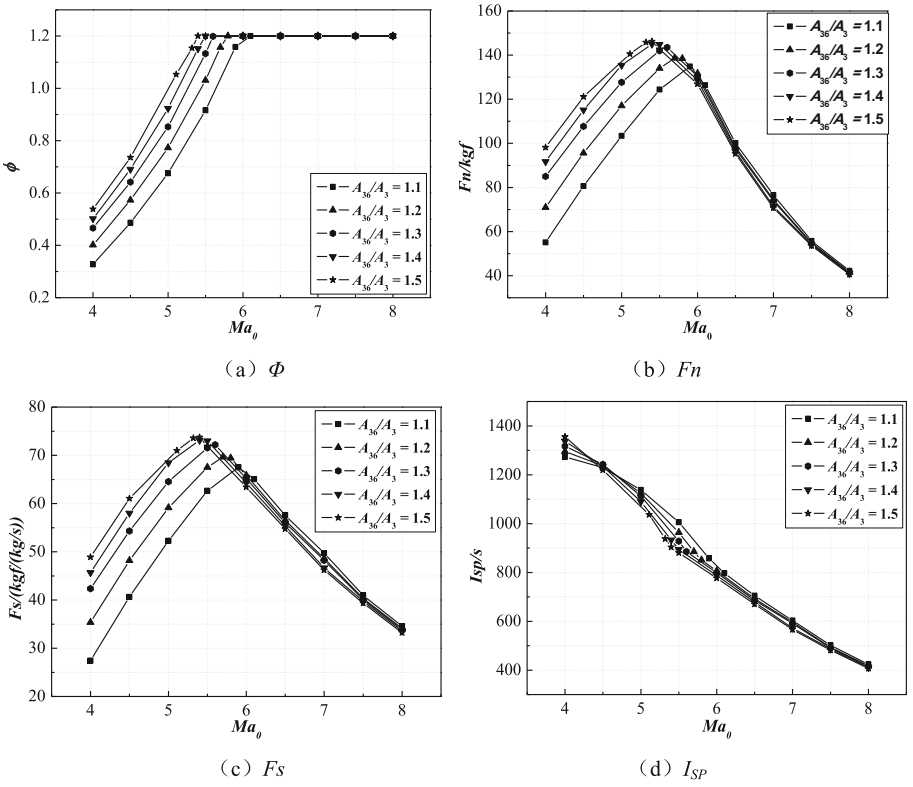

Fig. 3. Effect of A_{36}/A_3 expansion ratio of third section combustion chamber on engine performance

3.2 The Proportion of Fuel Supply to the Combustion Chamber

The expansion ratios of the three sections of the combustion chamber are 1.0, 1.4 and 2.0, respectively. The other configuration parameters are unchanged, and the fuel supply rate of the three-section combustion chamber is analyzed and compared according to the following five conditions. The detailed fuel supply ratios in the five cases are shown in Table 3. The engine is operated at maximum fuel supply, and the overall performance of the engine at different flight speeds is calculated, as shown in Fig. 4.

Table 3. Distribution of fuel supply at each point of three-section combustion chamber

Num	Φ_1	Φ_2	Φ_3
1	0.20	0.25	0.55
2	0.20	0.30	0.50
3	0.20	0.35	0.45
4	0.20	0.40	0.40
5	0.20	0.45	0.35

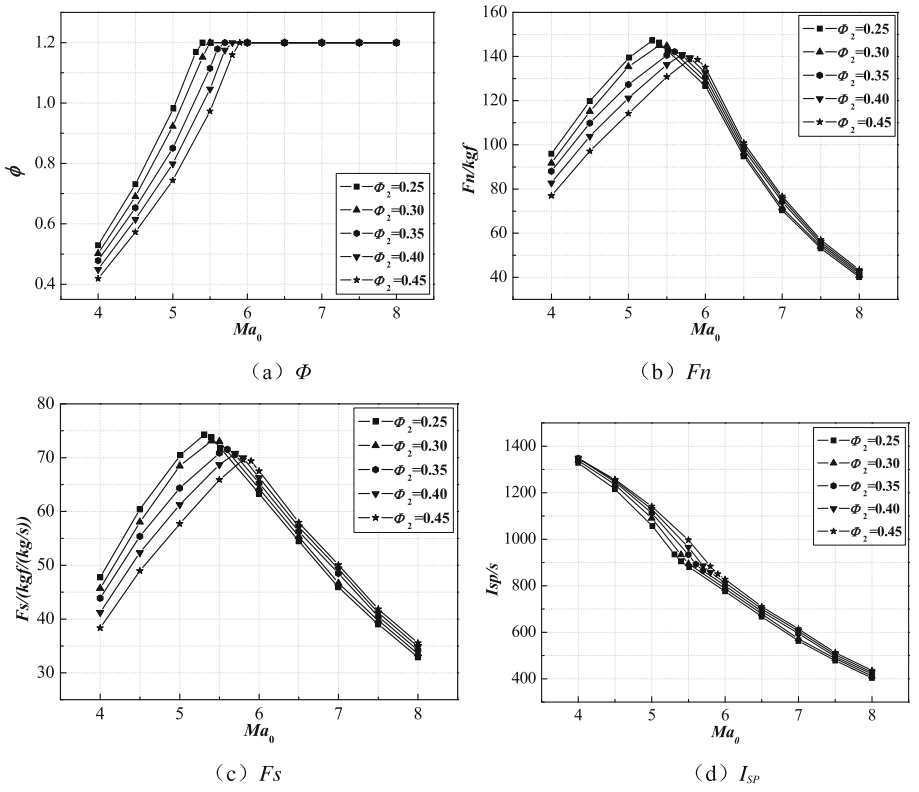

Fig. 4. The effect of the fuel supply ratio Φ_2 on the performance of the third section combustion chamber

From Fig. 4(a), it can be seen that for the same flight condition, when the maximum equivalent fuel-air ratio of the combustion chamber does not reach the equivalent fuel-air ratio Φ = 1.20, the maximum equivalent fuel-air ratio of the engine is reduced with the decrease of the second-section fuel supply ratio Φ_2 of the combustion chamber. This is because the fuel supply ratio Φ_2 of the second section of the combustion chamber is reduced, that is, the heat absorption of the gas upstream of the combustion chamber is reduced, the overall Mach number of the combustion chamber is increased

as a whole, and the thermal resistance loss during the heating process is increased. The Mach number downstream of the chamber decreases, but it is reflected in the geometric relation that the throat of the combustion chamber moves backwards, the area of the throat increases, and more fuel can be added in the combustion chamber. When the fuel supply ratio Φ_2 in the second section of the combustor is constant, the maximum engine thrust increases first and then decreases with the increase of the flying Mach number. The reason is that before the equivalent fuel-air ratio $\Phi = 1.20$, the engine equivalent fuel-air ratio, the increase in thrust leads to an increase in thrust; the reason for the next decrease in thrust is that the overall Mach number of the combustion chamber increases, the thermal resistance loss increases, and the combustion mode of the engine transitions to the purely scramjet mode direction in which the boundary layer is not separated; for the same in the flight condition, the maximum state thrust decreases with the increase of Φ_2 before the maximum equivalent fuel-air ratio of the combustion chamber reaches the equivalent fuel-air ratio $\Phi = 1.20$, but the maximum state thrust increases with the increase of Φ_2 when the equivalent fuel-air ratio $\Phi = 1.20$. However, the impact is not great. The engine specific thrust *Fs* and the thrust *Fn* have the same tendency (Fig. 4(c)). From Fig. 4(d) we can see that the specific impulse increases with the increase of the fuel supply ratio Φ_2 in the second section of the combustion chamber. The reason is that the larger the fuel injection quantity upstream of the combustion chamber, the higher the heat absorption in the upstream of the combustion chamber, resulting in an overall upper Mach number deviation low, the thermal resistance loss during heating decreases, and the total engine pressure loss decreases, so the engine specific impulse increases.

4 The Influence of Design Parameters of the Four Sections of the Combustion Chamber

To study the influence of the design parameters of the four-section combustion chamber, this section selects two variables for study: A_4/A_3, Φ_4. The parameter definition is similar to Fig. 1, in which A_4 is the fourth section of the combustion chamber exit area, and Φ_4 is the fuel supply rate of the fourth section combustion chamber.

4.1 The Geometry of the Combustion Chamber

The fuel distribution ratio of the four sections of the combustion chamber is kept constant at 0.20, 0.25, 0.25, and 0.30, respectively. The configuration of the following five cases with different expansion ratios is used, as shown in Fig. 5. Detailed configuration parameters are shown in Table 4. The engine is operated at maximum fuel supply, and the overall performance of the engine at different flight speeds is calculated, as shown in Fig. 6.

From Fig. 6(a), it can be seen that the expansion ratio of the fourth section of the combustion chamber has little effect on the maximum equivalent fuel-air ratio of the engine, because the configuration of the first three sections of the combustion chamber is certain, and the four-section fuel distribution ratio remains unchanged, making the combustion chamber thermal choke, the flow rate at the throat is constant, and the air

Table 4. Four-section combustion chamber expansion ratio

Num	A_{35}/A_3	A_{36}/A_3	A_{37}/A_3	A_4/A_3
1	1.0	1.2	1.3	2.0
2	1.0	1.2	1.3	2.2
3	1.0	1.2	1.3	2.4
4	1.0	1.2	1.3	2.6
5	1.0	1.2	1.3	2.8

flow already adheres to the fourth section of the combustion chamber, so the maximum equivalent fuel-air ratio remains unchanged. For the engine thrust, it can be seen from Fig. 6(b) that under the condition that the expansion ratio A_4/A_3 of the fourth section of the combustion chamber is not changed, the maximum state thrust of the engine increases first and then decreases with the increase of the flying Mach number $Ma_0 = 5.5$, the thrust of the engine reaches its maximum; for the same flight condition, it can be seen that the maximum engine thrust increases with the increase of A_4/A_3, because the air flow passes through the fourth section of the combustion chamber and is already an adherent flow. For the supersonic flow, in the expansion plane, the flow is accelerated, and the larger the expansion angle is, the faster the air flow is accelerated. The engine specific thrust *Fs* and the thrust *Fn* change in the same direction, as shown in Fig. 6(c). For the engine specific impulse, it can be seen from Fig. 6(d) that the effect of the A_4/A_3 is not significant at the low Mach number flight because the maximum amount of fuel that can be added to the engine is small when the aircraft is flying at a low Mach number. So that the combustion chamber exit temperature is low, fuel heat dissociation can be ignored; while flying at high Mach number, the impact of A_4/A_3 is increasing, and the larger the A_4/A_3, the higher the engine specific impulse.

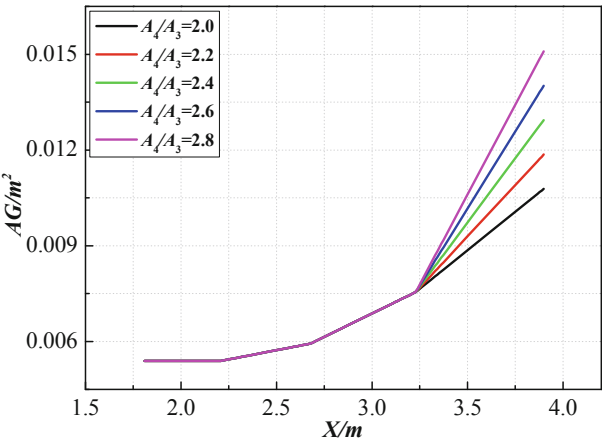

Fig. 5. Four-section combustion chamber with different fourth section expansion ratio A_4/A_3 configuration

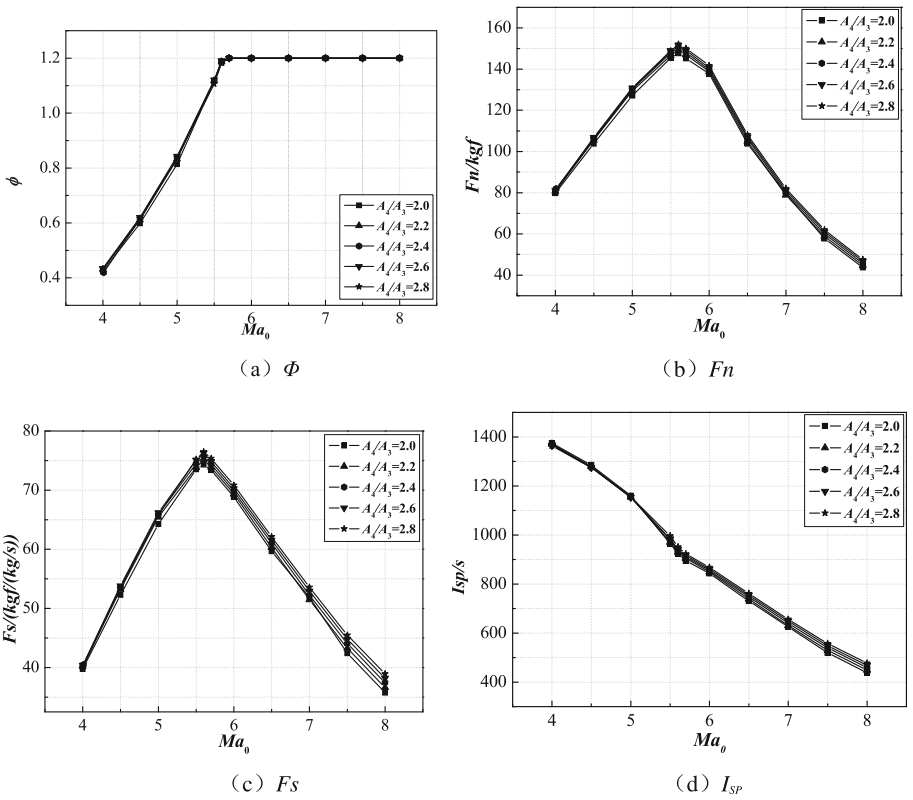

Fig. 6. Effect of A_4/A_3 expansion ratio on the fourth section combustion chamber on engine performance

4.2 The Proportion of Fuel Supply to the Combustion Chamber

In this section, the expansion ratio of the four sections of the combustion chamber is 1.0, 1.2, 1.3, and 2.0, respectively, and the other configuration parameters remain unchanged. The fuel supply rate of the first three sections of the combustion chamber remains unchanged, and only the fourth section of the fuel supply parameters is changed. According to the following five conditions (Table 5) for analysis and comparison, the engine is operated at maximum fuel supply, and the overall performance of the engine at different flight speeds is calculated, as shown in Fig. 7.

Table 5. Distribution of fuel supply at each point of four- section combustion chamber

Num	Φ_1	Φ_2	Φ_3	Φ_4
1	0.20	0.25	0.25	0.30
2	0.20	0.25	0.25	0.35
3	0.20	0.25	0.25	0.40
4	0.20	0.25	0.25	0.45
5	0.20	0.25	0.25	0.50

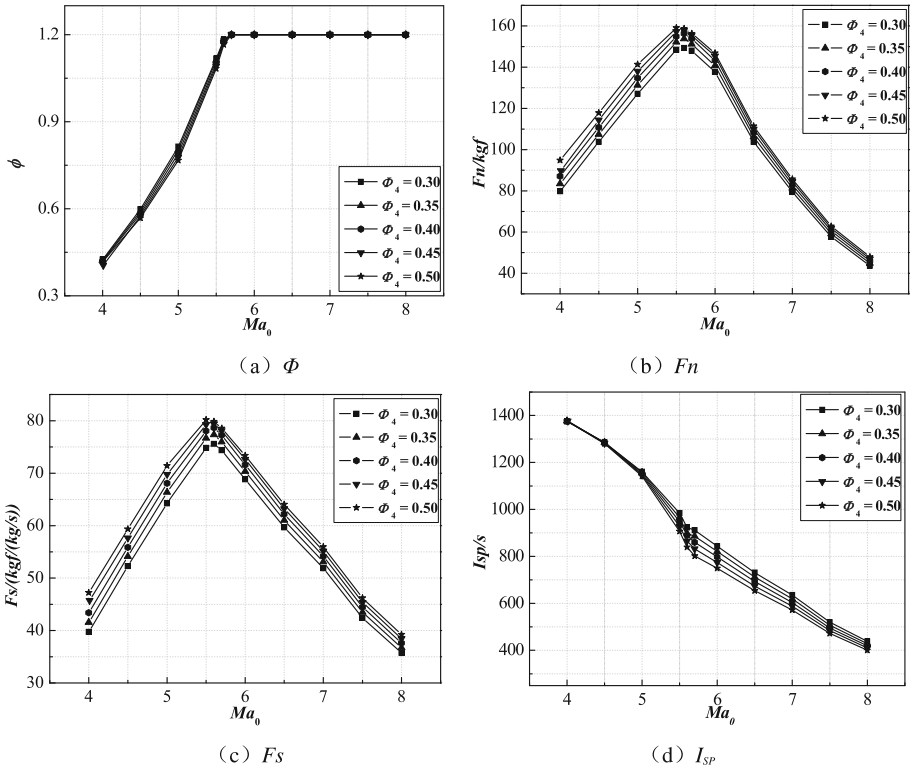

Fig. 7. The effect of the fuel supply ratio Φ_4 on the performance of the fourth section of a four-section combustion chamber

From Fig. 7(a), it can be seen that for the same flight condition, the fuel supply ratio Φ_4 in the fourth section of the combustion chamber has little effect on the maximum equivalent fuel-air ratio of the engine because the parameters of the inlet air flow are unchanged, and the configuration of the four-section combustion chamber is certain, and before the three-section fuel distribution ratio does not change, so the flow in the first three sections of the combustion chamber is almost the same, and the thermal throat of the combustion chamber often appears in the straight section of the combustion chamber and the first expansion section, so the geometric area and flow rate at the thermal throat are not change, so the maximum equivalent fuel-air ratio does not change. Under the condition that the fuel supply ratio of the fourth section of the combustion chamber is constant, the maximum equivalent fuel-air ratio of the engine appears to increase first and then remain unchanged with the increase of the flight Mach number; for the engine thrust, as shown in Fig. 7(b), When the fuel supply ratio Φ_4 in the fourth section of the combustion chamber is constant, the maximum engine thrust increases first and then decreases with the increase of the flight Mach number Ma_0, reaching the maximum at Ma = 5.5; for the same flight condition, we can see that the thrust of the engine increases with increasing Φ_4, and at low Mach numbers, Φ_4 has a

greater influence on the engine thrust and has a smaller effect at high Mach numbers because the flow velocity of the combustion chamber is slower at low Mach numbers, although the fuel injected into the fourth section of the combustion chamber is more, but most of the fuels are burned completely and the combustion efficiency is high. Therefore, Φ_4 has a greater influence on the engine thrust; however, at high Mach numbers, although the combustion chamber adds more fuel, the airflow faster, the residence time of the fuel in the combustion chamber is shorter, and many fuels do not enter the nozzle directly without combustion, so the Φ_4 has little effect on engine thrust. As can be seen from Fig. 7(d), the specific impulse decreases as Φ_4 increases, and the influence at low Mach numbers is small.

5 Conclusion

With the increase of the flight Mach number, the engine maximum thrust first increases and then decreases. When $Ma_0 = 5.5$, the thrust of the engine reaches its maximum.

Through the study of different geometric configurations and fuel injection methods, it is found that increasing the thermal throat area of the combustion chamber can effectively increase the thrust of the aircraft during low-speed flight.

In the case where there is no thermal choking and no influence on the intake start, increasing the fuel distribution ratio in front of the combustion chamber and the length of the expansion section can improve the specific impulse at high engine speed.

References

1. White ME, Drummond JP, Kumar A (1986) Evolution and status of CFD techniques for Scramjet applications. In: Joint technology office of hypersonics. Roadmap for the hypersonic programs of the department of defense. Pub. L. No. 109-364, AIAA 1986, p 00160
2. Heiser WH, Pratt DT, Daley DH, Mehta UB (2002) Hypersonic Airbreathing Propulsion. AIAA education series
3. Cockrell CE, Auslender AH, Wayne Guy R (2002) Technology roadmap for dual-mode Scramjet propulsion to support space-access vision vehicle development. In: AIAA 2002, p 05188
4. Hirschel EJ, Erbland PJ Critical technologies for hypersonic vehicle development. RTO-EN-AVT-116
5. Pamadi BN, Brauckmann GJ (2001) Aerodynamic characteristics, database development, and flight simulation of the X-34 vehicle. In: AIAA 2001, p 03706
6. Faulkner RF, Pratt, Whitney (2003) The evolution of the HYSET hydrocarbon fueled Scramjet engine. In: AIAA 2003, p 07005
7. Waltrup PJ, White ME, Zarlingo F (2002) History of U.S. Navy Ramjet, Scramjet, and mixed-cycle propulsion development. In: AIAA 2002, p 05928
8. Prisell E (2005) The Scramjet - a solution for hypersonic aerodynamic propulsion. In: AIAA 2005, p 03550
9. Ferlemann SM, McClinton CR, Rock KE (2005) Hyper-X mach 7 Scramjet design, ground test and flight results. In: AIAA 2005, p 03322

10. Hellman BM, Hartong AR (2007) Conceptual level off-design Scramjet performance modeling. In: AIAA 2007, p 05031
11. Mitani T, Tomioka S, Kanda T, Chinzei N, Kouchi T (2003) Scramjet performance achieved in engine tests from M4 to M8 flight conditions. In: AIAA 2003, p 7009
12. Heitmeir F, Lederer R, Herrmann O (1992) German hypersonic technology programme airbreathing propulsion activities. In: AIAA 1992, p 5057
13. Hass NE, Smart MK, Paull A (2005) Flight data analysis of HyShot2. In: AIAA 2005, p 3354
14. Wu X (2007) Research on design optimization of integrated flow passage for scramjet engine. Doctoral dissertation of National University of Defense Technology, p 10
15. Wang C (2011) Research on the overall design and optimization of Scramjet ramjet. National University of Defense Technology Ph.D. thesis, p 11